DESIGN OF AN INCLINED WEIGHT MEASUREMENT SYSTEM FOR PROSTHETIC ARM INNOVATION

Tran Dang Khoa, Nguyen Thanh Hai
Ho Chi Minh City University of Technology and Education, Vietnam

Received 7/8/2019, Peer reviewed 21/8/2019, Accepted for publication 26/8/2019

ABSTRACT

Force feedback is one of the top critical aspects of prosthetic solutions. For patients equipped with powered prosthetic arms, their ability to grasp, manoeuvre and feel heavy objects is limited at rest and during exercises. This research approaches a solution that may help to solve the problem for many patients – a prototype capable of measuring the weight of objects automatically at multiple degrees of freedom of the patient's prosthetic arm. By incorporating the existing technologies of a micro-electromechanical system capacitive accelerometer with a strain gauge force transducer, the weight of an object is measurable instantly the moment it is held, independent of any inclination. Results showed that the weight of an object measured at different 90^o movement angles is similar to the actual weight of the object in use. The mean measurement error is approximately ±0.05kg of the tested object's mass of 1.5kg at multiple inclines. Not only the result showed a positive outcome which fulfilled the objectives of the research, but it is also a deciding factor for developing the technology further. Apart from helping to improve patients' sensory feedback, one of its top applications in healthcare is monitoring patient prosthesis-compatibility during heavy exercises.

Keywords: *Inclined weight measurement; Prosthetics arm; MEMS accelerometer; Movement angles; Load cell.*

1. INTRODUCTION

Based on the national investigation results published by the General Statistics Office of Vietnam (GSO) and The United Nation of Children's Fund (UNICEF), in 2019, 7% of Vietnam's population (approximately 6.2 million) are people with disabilities. The disability count is increasingly higher worldwide, with the world population of amputees being 10 million in 2008 and, there are approximately more than 1 million limb amputations annually [1,2]. In particular, according to information provided by National Centre for Health Statistics, there are nearly 2 million amputees living in the United States and 200,000 more every year (with a 1:4 ratio of the upper limb to lower limb amputation); this number will double by the year 2025 [3,4]. In Vietnam, about 10,000 prosthetics, sponsored by Mercer on Mission, were fitted to amputees, estimated from 2009 to 2018 [5].

The major causes leading to limb amputation include cardiovascular diseases (54% diabetes and peripheral arterial disease), traumatic accidents (45%), infection, cancerous tumours, nerve injury and congenital anomalies (less than 2%) [2]. The number will be more concerning with more people being affected by those diseases. For example, the current global prevalence of diabetes will burgeon from 285 to 435 million people by 2030 [2]. In Vietnam, the number of limb disabilities is much higher, about 1 million disabled people and more, as a consequence of Agent Orange. An increasing number of amputation cases, as a result of severe injuries to various body parts, drives the demand for robotic prosthetics across the globe [6].

Our sense of touch is one of the primary means of interaction with our surrounding environment. Our biological sensory systems can easily communicate weight information of an object while holding or lifting the object using our biological limbs. However, for amputees with prosthetic limbs, their natural sensation is partially lost. For them, the loss of sensory feedback hinders the patients' abilities to perform daily activities, including the ability to hold and feel the weight of objects [7].

One of the top critical aspects of prosthetic solutions is force feedback. Some commercially available myoelectric prosthetic arms, for example, i-Limbs, Be-Bionic, and Michelangelo are integrated with tactile sensory systems to measure forces of contact, sliding and temperature. However, they all lack an essential capability of measuring and sensing the weight of holding an object, especially heavy objects, which could potentially solve multiple problems experienced by prosthetic users [8]. Hence, this research will suggest a simple and innovative solution by developing a technology capable of measuring the mass of lifted objects at multiple angles and directions.

The key technique here is to combine the functions of both the electrical force transducer which gauges the weight of objects in the gravitational direction and an analogue accelerometer which measures the angle of inclination of the arm. By processing both measurements with a pre-programmed microprocessor, the calibrated weight of the object can be computed automatically. Accelerometers have often been used for controlling industrial robotic arm [9-10]. One of the researches, conducted by two prosthesis experts, Peter Kyberd and Adrian Poulton, has shown that accelerometers can be used to augment the control of powered prosthetic arm by detecting the orientation of the limb and correcting the amount of torque required to move the limb [11]. In another research, Joan Sanders has successfully used a modular six-directional force and moment sensor to assess prosthetic's performance [12]. Moreover, Edward Neumann has been able to use a load cell and force-moment curve to directly measure and evaluate the transverse plane loading moment on transtibial residual limbs [13]. All the force, moment and accelerometer sensors used above-provided complex functionality with high accuracy and precision in controlling and monitoring the prosthetics. However, the systems are costly and not so flexible to be integrated with some existing prosthetics.

While accuracy, precision and repeatability of sensors are imperative in prosthetic applications, price is, nonetheless, another important factor to consider in the healthcare industry [7-8]. Hence, the objective of this paper assesses the feasibility of using a combination of inexpensive, conventional load cell and accelerometer to measure movement force based on prosthetic orientation. This paper covers the construction of the inclined weight measurement system. Weight and angle signal will be processed and analysed using descriptive statistics. The measurement result was made visible on a liquid crystal display (LCD) and a computer monitor. Experimental results are independent of any human trial on sensory feedback. The experiment took place with the entire circuit being mounted on a mechanical structure which resembles the shape of a prosthetic arm. The success of the paper led to considerations of possible existing designs of prosthetic arms to fit the instruments, the likely expansion of the research, and the applications of the technology to other disciplines.

2. MATERIALS AND METHODS

2.1. Data Acquisition and Signal Processing

For the design of this system, many high technology devices were used, such as MMA8452Q tri-axis Micro-electro Mechanical Systems (MEMS) capacitive accelerometer, Bi-directional Logic Level

(LLC) converter/shifter and HX711 Load Cell Amplifier (LCA) breakout boards and Liquid Crystal Display (LCD) module, an Arduino UNO development board, an aluminium strain-gauge load cell. Moreover, open-source software includes Microsoft Word, Excel and Arduino Integrated Development Environment (IDE), Fritzing and National Instruments (NI) Multisim.

2.2. Structure of Inclined Weighing System

The main steps of the proposed methodology to inclined weight measurement is shown in ***Fig. 1***, in which the block diagram of the system illustrates the entire process of acquiring, conditioning, processing, and displaying measurements of signal data.

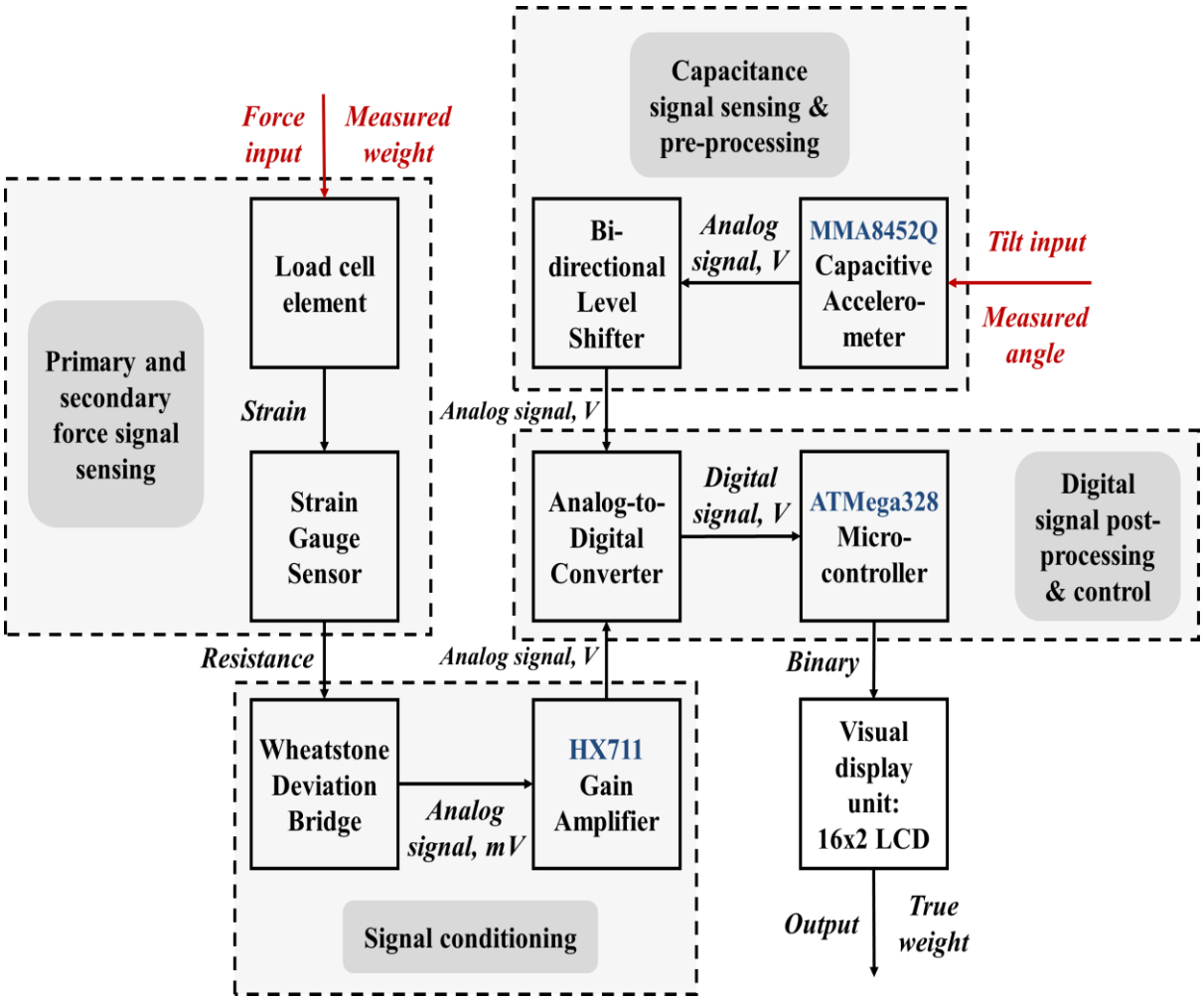

Fig. 1 *Functional block diagram of a general structure of the inclined weighing system.*

In ***Fig. 1***, the load cell and accelerometer will communicate over either analogue or digital connection interface. The analogue signal is then amplified and converted to digital signals by an Analogue-to-Digital Converter (ADC) on the Arduino. Digital signal will then be processed and displayed accordingly.

2.3. Methodology

The first simple experiment involved the use of a fixed weight which was attached to the pulling end of a spring-loaded Newton meter. The force measured by the Newton meter changed when changing the angle of measurement. Besides, this change in force values can be calculated using mathematical

equations. The similarity between physical measurements and calculated values confirmed the feasibility of the paper.

The second experiment required automated force measurement using an electronic system which includes an accelerometer and a force transducer, as mentioned previously. The experimental prototype was built on a breadboard with premade breakout boards with built-in sensors that can be controlled by the Arduino. The Arduino development board controls the flow and processing of sensors' data. ***Fig. 2*** describes the programming process by which data is acquired and calibrated:

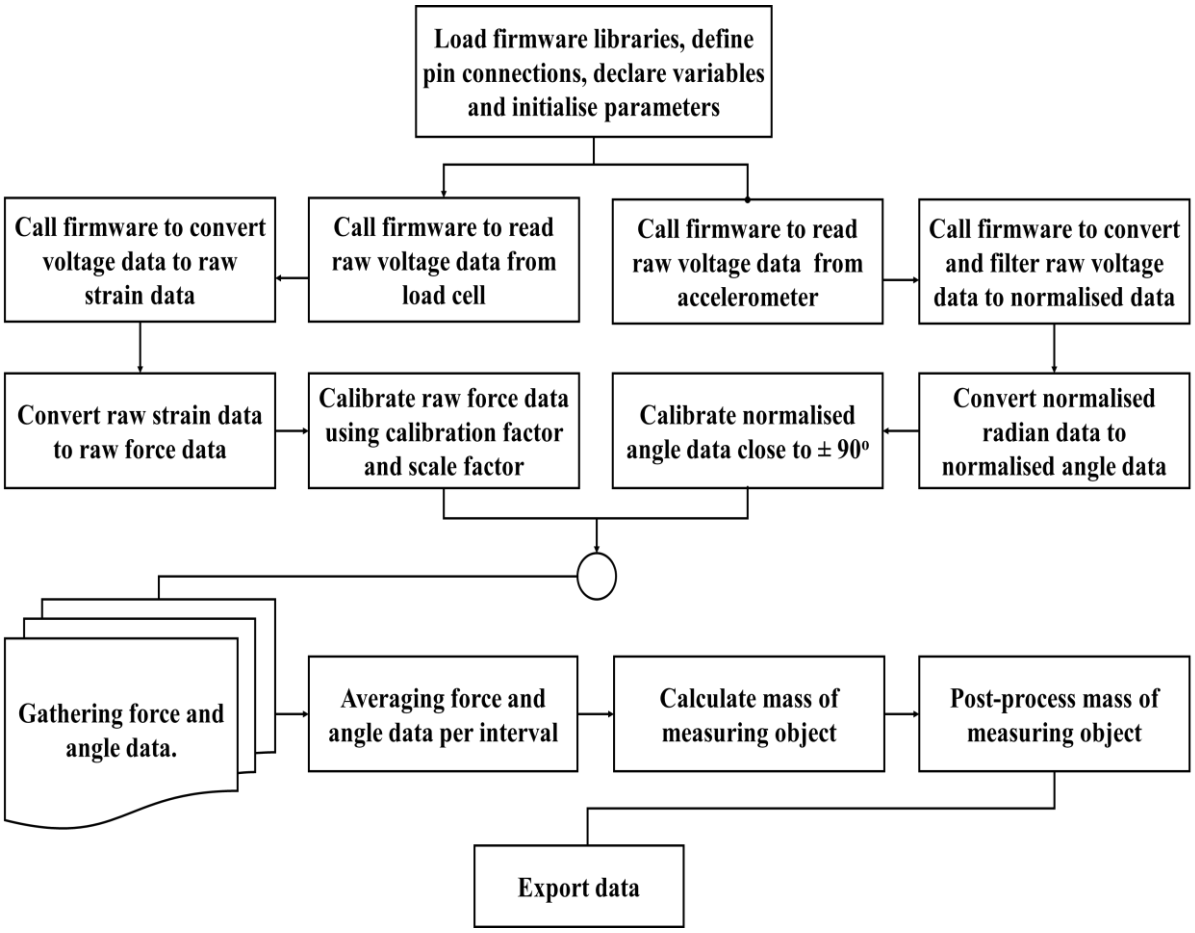

Fig. 2 *Block diagram of a multi-sensor based inclined weight measurement system.*

In addition, details on the calculation and calibration of force, angle and mass of measuring object are described in this paper.

2.3.1. Force Measurement Configuration

The force measurement process comprised of force sensing and force transduction. Resistive force measurement technique was chosen for the advantages regarding size, price, accuracy, reliability and ease of use. More precisely, a resistive strain-gauge force transducer, sometimes called resistive strain-gauge load cell, in which its working principles were based on a resistive measurement method, was used [14]. ***Fig.* 3** shows the configuration of the force measurement unit, including a middle-bending element with two embedded ends, connections between aluminium load cell, two strain gauges and one HX711 load cell amplifier.

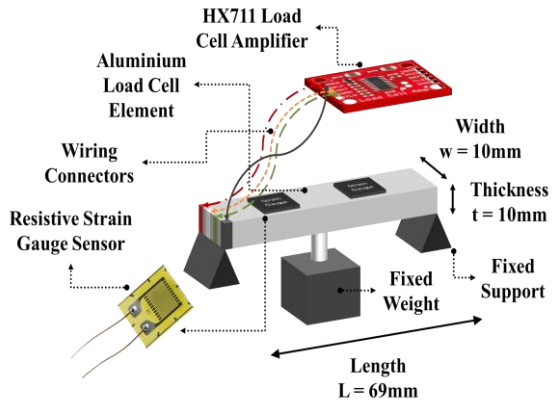

***Fig. 3** Illustration of a force measurement unit using an aluminium load cell, two strain gauges and one load cell amplifier.*

In ***Figure 3***, the force measurement unit comprised a central-bending aluminium alloy load cell element with a set of two biaxial strain gauges mounted on top of an elastic aluminium alloy element. The strain gauges were conducting device for measuring the changes in strain, due to deformation or elongation under an applied force, in distances between points in the load cell. When the load cell element deforms or elongates, induction of strain on the load cell produces a change in electrical resistance of the strain gauges (piezoresistive property). The change in electrical resistance takes place due to the change in the resistive element dimensions as well as in the material resistivity [15].

The change in electrical resistance is measurable using a Wheatstone half-bridge circuit and a set of programmable equations based on the physical principles of the selected load cell. Strain gauges for this experimental setup have their length placed parallel to the direction of tensile force acting on both ends the load cell, as to receive maximum sensitivity. A bending force applied at the centre of the element will stretch the strain gauge. The conductive wires of both strain gauges become narrower and longer while their resistance increases due to the applied tension on both gauges. The specified load limit for this specific load cell is approximately 500N, and the load range for this type of load cell's configuration is between 10^1 to 10^4N [16].

Based on the configuration of the load cell (a fixed–fixed centre load beam), the theoretical strain, ε_{theory} ($\mu\varepsilon$), is derived from Hook's law and Euler's second law as follows [17]:

$$\varepsilon_{theory} = \frac{L^2}{12\delta.y} \quad (1)$$

where L (m) is the length of the load cell element, δ (m) is the elastic deflection of the load cell element, and y (m) is the vertical distance away from the beam's neutral axis.

Values of theoretical strain can then be used to compare with practical measurements, which can be derived from the perpendicular axis theorem and Euler's second law, which calculated the theoretical force, F (N) acting on load cell element as follows:

$$F = \frac{\varepsilon.E.t.w}{3L.y}.(t^2 + w^2) \quad (2)$$

where E (Pascal) is Young's modulus based on the load cell's material; t (m) and w (m) are the thickness and width of the load cell element, respectively.

For all practical measurements, experimental strain for a half-bridge circuit can be computed as the following equation [14, 17, 18]:

$$\varepsilon_{experimental} = \frac{2V_{out}}{k.V_{in}} \quad (3)$$

where V_{out} (mV) is the output voltage when a load is applied, V_{in} (mV) is the input voltage of the strain gauge, k is the gauge factor of half-bridge circuit.

2.3.2. Angle Measurement with Micro-Electromechanical Systems Capacitive Accelerometers

Accelerometers, in general, detect and measure a vector quantity of proper acceleration. Micro-Electromechanical System (MEMS) capacitive accelerometers

are preferable for the paper as it is most suitable for this research regarding its functions, size, cost, accuracy and repeatability. However, they are prone to the noise level, sensitive to the electromagnetic field, and more complex to use in electronic designs. Applications of these accelerometers include vibration, shock detection, inertial navigation and tilt sensing.

The accelerometer can measure both static and coordinate acceleration due to gravity, or dynamic and proper acceleration such as vibrating motion. Measurement vectors are obtainable on up to three axes, X, Y, and Z. The analogue output signal is a sine wave that is presented as acceleration (rate of change of velocity) or g-forces (with a dimension of a metre). During the experiment, values of acceleration and g-force are calculated from capacitance or voltage outputs by the pre-programmed firmware. These values were used to calculate the orientation angles of three-axis accelerometer and the equations are described as follows [9,19]:

$$\theta_1 = \tan^{-1}\left(\frac{X}{\sqrt{Y^2 + Z^2}}\right) \quad (4)$$

$$\theta_2 = \tan^{-1}\left(\frac{Y}{\sqrt{X^2 + Z^2}}\right) \quad (5)$$

$$\theta_3 = \tan^{-1}\left(\frac{\sqrt{X^2 + Y^2}}{Z}\right) \quad (6)$$

where θ_1, θ_2 and θ_3 (degrees) are the orientation angles of the accelerometer in X, Y and Z planes; X, Y and Z are values of acceleration or g-force. The gravity acting on the x-axis is a sine function while that acting on the y-axis is a cosine; therefore, the ratio between two axes gives a tangent.

2.3.3. Combining Force and Angle Data

The working principles behind the inclined weighing system combine both the sensing technologies of the accelerometer and force transducer, which are illustrated in ***Figure 4*** and ***Figure 5***:

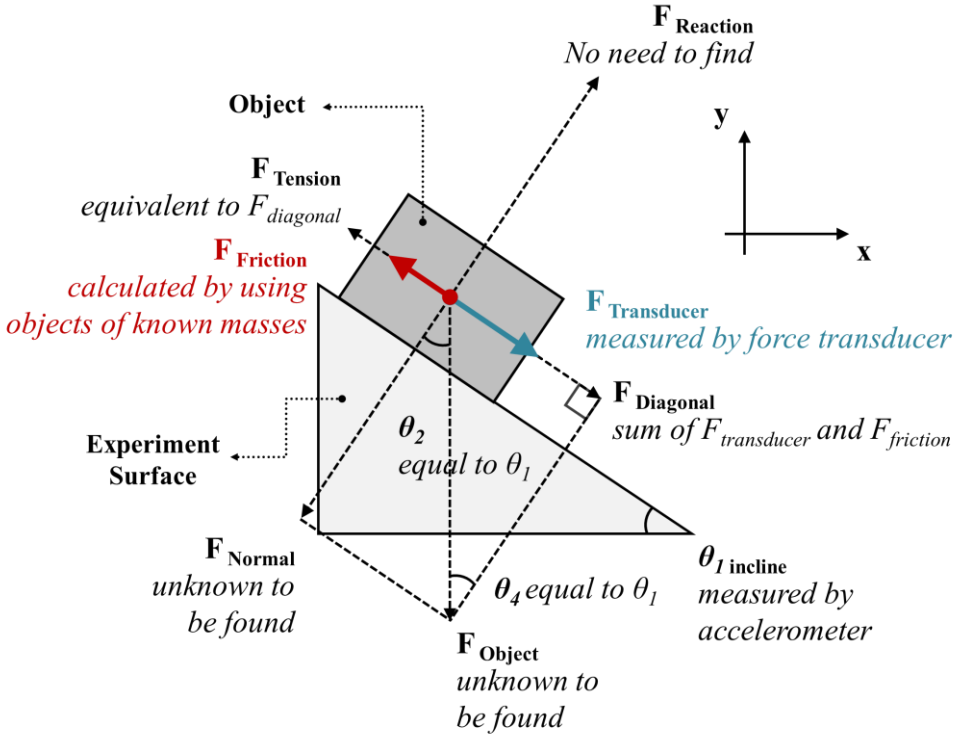

Fig. 4 *Free-body force diagram showing the physical principles of the entire system, in which calculations are based on geometrical physics.*

Figure 4 shows a free-body diagram of forces acting on the rectangular object held stationary on a slope by a string while ***Figure 5*** describes a free-body diagram of the technology applied on the prosthetic arm. The friction force, F (N), is only accountable in ***Figure 4*** and neglected on the other. The reason for this difference is due to the setup difference. Measuring object in ***Figure 5*** is not placed on a sloped surface but instead being held by the robotic arm. The deformation of the load cell by the object's mass is not subjected to any surface friction effect. The working principle for the prototype setup is mainly based on ***Figure 4***, which is slightly more complicated. The simple Law of Sine governs the working principles on both models, with or without friction, respectively. Therefore, F (N) is the force calculated as follows:

$$F_0 = \frac{F_T}{\sin\theta} \rightarrow m_0.g = \frac{F_T}{\sin\theta} \rightarrow m_0 = \frac{F_T}{g.\sin\theta} \quad (7)$$

where m is weight (N), θ is tilt angle (radians), μ is surface's friction coefficient, and g = 9.81 ($m.s^{-2}$) being gravitational acceleration.

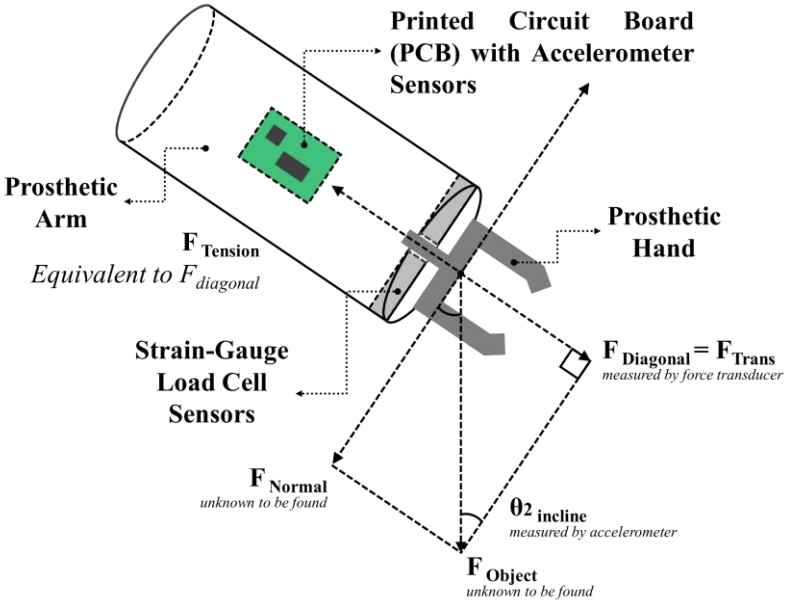

Fig. 5 *Free-body diagram showing the working principle of a prosthetic arm*

In ***Figure 5***, without friction, $F_D = F_T = F_{TE}$. Object's inertial mass is calculated using the object's relative force, $F_{Transducer}$ sensed by a load cell and tilt angle, θ measured by the accelerometer. With $F_D = m_o.g.\sin\theta$, $F_N = m_o.g.\cos\theta$, and $F_f = \mu.F_N$, substitute all F_D, F_N, and F_f and equations which are only valid for force measurement in one plane, y-plane satisfying the requirements of the research are denoted as follows:

$$F_D = F_{TE} = F_T + F_f \quad (8)$$

$$\rightarrow m_0 = \frac{m_T}{\sin\theta - \mu.\cos\theta} \quad (9)$$

When friction is accounted, the friction coefficient of the slope surface can be found using the following equation:

$$\rightarrow \mu = \frac{m_0.\sin\theta - m_T}{m_0.\cos\theta} \quad (10)$$

2.3.4. Filtering and Calibrating Signal Data

The MMA8452Q chips are calibrated at the factory to a level of precision sufficient for most purposes. The signal data is pre-processed by the accelerometer's built-in low-pass and high-pass filters with different pre-programmed measurement ranges.

However, a further calibration technique is required for a more accurate measurement. One of the basic methods is to take measurements in ±1g field and the actual output amplitudes are determined using Equation (11) [19]:

$$A_{actual} = \frac{A_{out} - [0.5(A_{+1g} + A_{-1g})]}{0.5\left(\frac{A_{+1g} - A_{-1g}}{1g}\right)} \quad (11)$$

where A_{actual} (g) is the exact acceleration acting on an accelerometer, A_{out} (g) is the accelerometer's output amplitude and $A_{\pm 1g}$ is the amplitude placed in the ±1g field.

The technique determined the sensor's output for each axis (up to three axes for tri-axis accelerometer) when they are precisely aligned with the axis of the gravitational force. The accelerometer was mounted onto a rotatable block, and acceleration measurements in ±1g field were taken for each axis of the sensor to form a calibration sketch. From the sketch and Equation (11), a scale factor was obtained for each axis.

3. RESULTS AND DISCUSSION

3.1. Prototype Setup

The electronic prototype was set up with some main components with the addition of a 10Ω potentiometer to adjust the LCD screen brightness and a 220Ω resistor with a wiring diagram, as shown in ***Figure 6***. Furthermore, signal amplification is required for the strain-gauge load cell, which done by using the HX711 breakout board with an amplifier circuit. Moreover, the board is also packed with 24-bit ADC converter with on-chip Programmable Gain Amplifier (PGA), power supply regulator, oscillator and a Power-On-Reset (POR) generator. The HX711 load cell amplifier circuit consisted of a Wheatstone half-bridge with 4 I/O pin to connect to the load cell. The pins are labelled and coloured RED, BLK, WHT, GRN and YLW. Each colour corresponds to the conventional colour coding of load cells: RED (Excitation+ or VCC) BLK (Excitation- or GND) WHT (Amplifier+, Signal+ or Output+) GRN (A-, S- or O-) and YLW (Shield). In this circuit, load cell calibration was done by testing a calibrated load against multiple calibration factors.

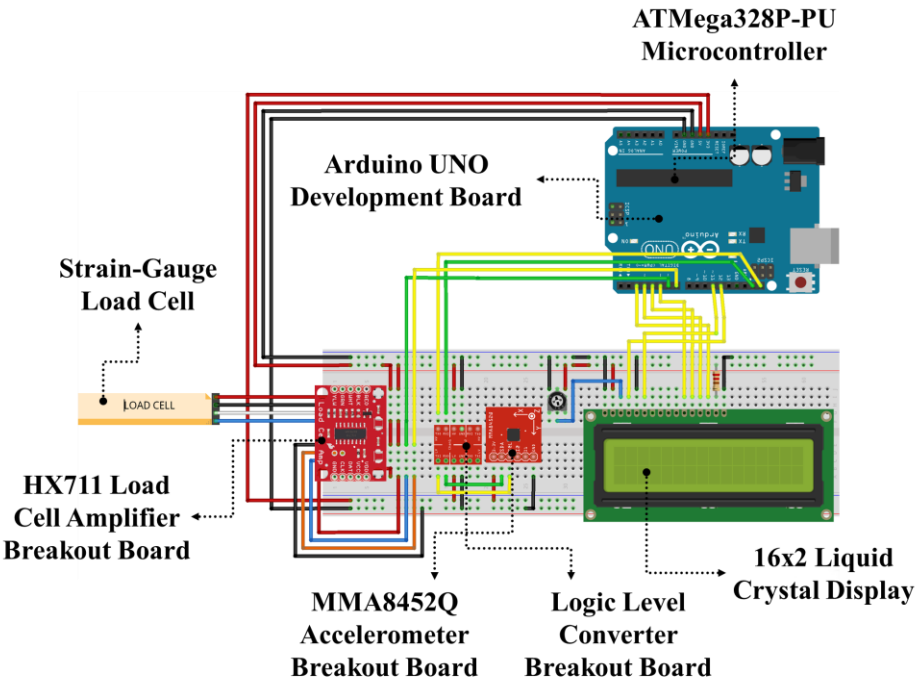

Figure 6. *Wiring diagram for an experimental prototype breadboard circuit*

The Arduino UNO supplies a 5-volt DC to the upper power rails of the breadboard and 3.3-volt DC to the bottom power rails. The accelerometer and logic-level converter are wired to 3.3V power supply while other components are wired to the 5V supply. Serial (SDA) and Clock Data (SCL) of both load cell amplifier and accelerometer are wired to SDA and SCL pins on the development board. For the load cell, four standard wires of Wheatstone bridge construction have four corresponding colours with each connecting to the correct amplifier's pins. Then, the complete system was attached to an acrylic plank, representing the overall shape and sizes of a prosthetic arm and acting as a surface to support the calibration weight.

3.2. Calibration and Measurement Results

Under the assumption that the ideal gravity is 1g, accelerometer's sensitivity decreased with the increase in orientation angles. Values read zero as the angle approached ±90°, and reading accuracy diminished significantly from above ±45° orientation. By reading two axes simultaneously, this sensitivity error can be compensated. The loss of sensitivity in one axis (with increasing inclination) was compensated by the increased sensitivity on the other axis (with decreasing inclination). However, a full spherical rotation of the dual-axis accelerometer will produce lower resolution and accuracy due to the internal construction of the MEMs. Hence, a calculation method using all three axes were applied in this research.

The accelerometer was observed to have a ±1^o offset. Calibration of this offset was possible if each axis of the accelerometer precisely aligned with the axis of gravitational pull. This calibration problem could effectively be resolved by using highly accurate electronic spirit levels or precision position jigs. Therefore, all measurements are assumed with a zero angle offset. The sensor alone provided precise measurements with only some readings having a deviation of ±5^o max. Since there was no big jump in measurement while the accelerometer was stationary, calibration was not required but instead, smoothing technique was applied where the average of every 100 readings was taken. The results were measurements with very low tolerance of ±0.1^o. Having said that the deviation after smoothing was infinitesimal, due to the combined effect of offset error and sensitivity mismatch error, the actual deviation from the accurate value can be beyond the accepted limits in inclination sensing application. Hence, calibration is required in future work when the required equipment is available to measure the errors.

The calibration factor for the strain-gauge load cell was found to be between -8,000 to -16,000. A known mass was loaded onto the load cell where changing the calibration factor will match the measured mass with the known mass. As load cell produced jumpy values of very large deviation even after the primary calibration, a second step to calibrate these values are required to remove any reading with large error. The technique required the code memorize all readings while constantly taking the cumulative average for every new reading. The mean reading was recorded constantly with a standard deviation calculated over time. If a large deviation occurs suddenly, that reading is automatically excluded from measurement. One of the apparent drawbacks of using cumulative data logging is high memory usage, high power consumption and lengthy calibration time.

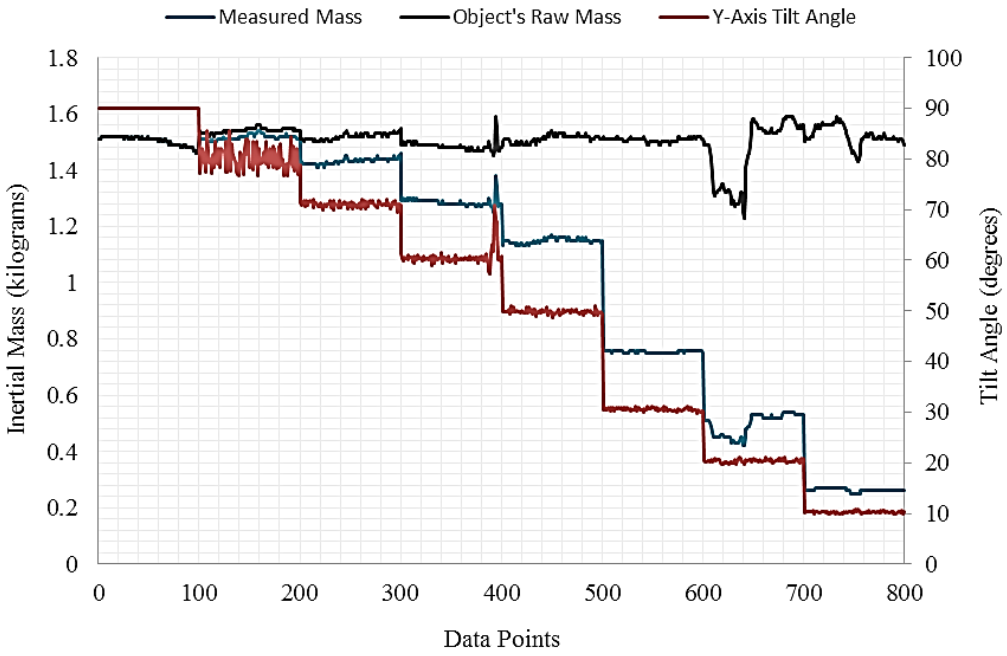

***Figure 7**. An illustration showing the calculated mass of the calibration weight (top black line), the measured weight (middle blue line) and the tilt angle of the system (bottom red line).*

As seen in ***Figure 7***, the experiment used a 1.5 kilograms (kg) calibration weight for measurement. Noted that the test was done using multiple objects of various weights, but only a 1.5 kg weight is confidently mentioned here because the weight is calibration standard – precisely 1.5 kg with insignificant tolerance. The calibration weight is costly due to its high accuracy, and no other standard weights were used due to the budget of the project. The mass was attached to the load cell, and the system is manually tilted and paused at different angles, starting from 90^o angle and slowly reduced to 10^o angle, with a step of -10^o each time. Logging of measurements was done at each degree step for 30 seconds. The data logging speed is set to 10 readings per second. The recorded data was exported to MS Excel, and a random range of 100 data points at each tilt angle was selected. The three lines from ***Figure 7*** represent calculated mass, measured weight and y-axis tilt angle, from top to bottom, respectively.

From ***Figure 7***, the overall pattern suggests that as the tilt angle becomes smaller, the weight readings are then reduced linearly. The calculated mass is the mass of the calibration weight computed using Equation (9) in Section 2.3.3, which remained constant over time with acceptable fluctuation. As the accelerometer's signals are filtered, and its data were calibrated, there is minimum fluctuation in the tilt angle measurements. However, between data points 80 and 220, there are significant fluctuations in signal data. This noisy signal event usually happened during a dynamic movement of the system every time the acrylic plank (where the system is attached to) is shifted to another tilt angle. Other subjective causes, based solely on assumptions, could be due to an electrical surge in the system or loose wiring during movement. The tilt angle, from data points 0 to 100, shows a constant value as the prototype was placed statically at 90^o angle. At this point, the mass of the calibration weight is equal to the measured weight of

itself; however, with small differences. Between data points 60 to 100, the angle data is constant while both the calculated mass and the measured weight slowly reduced over this period. This phenomenon can be explained by the theory of creep and hysteresis of the load cell, which is outside the scope of this article. Apart from that, the measured weight values are constant at each tilt angle. However, it does not mean that there is no creep effect at each tilt angle. Because random ranges of data points were selected, creep effect may not be observed for the data chosen. At 30^o tilt angle, a significant fluctuation of measured weight, between data points 600 and 660, is the due to infrequent noise from the load cell. This noise was not filtered using any firmware or software. Moreover, it is noticed that, between data points 600 to 800, noise signals are becoming more apparent in the calculated mass data. This is due to higher sensitivity at lower tilt angle and amplification of noise signal due to Sin(θ) approaching lower value on the sine curve. Sin(θ) is inversely proportional to the calculated mass. Throughout the experiment, friction was infinitesimal for θ^o ranging from 90^o to 20^o and was significant in the tilt region of 0–20^o, giving large error in measurements. The limitation of the prototype setup is that it could not measure the load at 0^o inclination (perpendicular to the gravitational field) and is restricted to the low 180^o of the 360^o spatial sphere. Shown in Table 1 below are the means and standard deviations of calculated masses at different tilt angles.

***Table 1**. Mean and standard deviation of calculated mass at different angles.*

Angle, θ^o	90	80	70	60	50	40	30	20	10
Mean Weight (kg)	1.50	1.54	1.52	1.49	1.51	1.54	1.51	1.46	1.52
Standard Deviation	0.02	0.01	0.01	0.02	0.01	0.02	0.01	0.11	0.03

From Table 1, the maximum measurement tolerance in the experiment was ±0.05kg (±3.3%) with the largest standard deviation of ±0.11 for a mean mass of 1.51 kilograms with mean tolerance of ±0.02kg.

3.3. Bionic Arms – System Incorporation

Inclined weighing system can be designed to fit the existing prosthetic arms on the market. Top considerations in the prosthetic design are size, power dissipation, accuracy and reliability. One of the challenges here is how to minimise the power consumption of sensors, the MEMS accelerometer and the force sensor. In order to save power, the electronic system can be altered to wake up and power sensors only when motion is detected.

More importantly, it is the design of the load cell that would fit the prosthetics easily. Depending on the types and application purposes of the load cell, it can be fabricated in different shapes, forms and sizes with a wide range of materials, producing load cells with different physical properties. A tension/compression load cell is preferable for the application compared to the bending beam load cell used in the prototype as the chosen prototype setup is highly unreliable to measure tension and compression alternatively as the bionic arm moves [15,20].

Compared to this prototype, which could only measure an object's mass lying within the bottom sphere of the 360^o spatial movement, the tension/compression load cell allows more freedom of measurement for the arm. It could effectively measure compressive force from above the neutral axis (above 0^o). Besides, the system can be designed to interact effectively with other existing sensors on prosthetic arms, like torque and pressure sensors. Furthermore, the inclined weighing system can be packed into a small, flexible printed circuit board (PCB), which can easily fit the arm internally or can be attached outside the arm [21].

4. CONCLUSION

This paper shows a real system for measuring inclined weight for prosthetic arm using the MEMS accelerometer and the bending load cell. This system was completed and could measure masses attached to a prosthetic arm at different tilt angles below the horizontal neutral axis. The mass measurement results showed only a small error of ±0.05kg (±3.3%). In conclusion, considering all the sources of noise for a relatively cheap prototype setup, the results achieved the overall aim of the research proving the feasibility of further investment in the paper to develop further, the technology that is fully functional for prosthetic arms as well as any other applications.

ACKNOWLEDGEMENT

With deep gratitude and admiration for all the help and support from Professor Paul Rees, Doctor Mark Holton, Mister Dave Moody and Mister Gareth Evans. Moreover, a sincere thank-you to Ho Chi Minh City University of Technology and Education and anyone who helped make this research possible.

REFERENCES

[1] C. D. Nguyen, T. H. Nguyen, "Launch of Key Findings of Viet Nam's First Large-Scale National Survey on People with Disabilities," *United Nations International Children's Emergency Fund*, Jan 10, 2019. [Online]. Available: https://www.unicef.org. [Accessed: Jul. 23, 2007].

[2] H. Claessen, M. Narres, B. Haastert, et al., "Lower-extremity amputations in people with and without diabetes in Germany, 2008–2012 – an analysis of more than 30 million inhabitants," *Journal of Clinical Epidemiology*, vol. 10, pp. 475–488, 2018.

[3] K. Ziegler-Graham, E. J. MacKenzie, P. L. Ephraim, T. G. Travison, and R. Brookmeyer, "Estimating the Prevalence of Limb Loss in the United States: 2005 to 2050," *Archives of Physical Medicine and Rehabilitation*, vol. 89, no. 3, pp. 422–429, 2008.

[4] M. F. Owings and L. J. Kozak, "Ambulatory and inpatient procedures in the United States, 1995," *Vital Health Stat 13*, vol. 135, pp. 1884–1891, 1998.

[5] K. Sears, "Mercer on Mission Fits 10,000th Vietnamese Amputee with Patented Leg Prosthetic," *Mercer University*, Jun. 26, 2018. [Online]. Available: https://news.mercer.edu [Accessed Jul. 23, 2019].

[6] MarketWatch, "Robotics Prosthetics Market 2018 Rising with CAGR of 9.5% Up To 2027 | Increasing Demand for Robotics Prosthetics Accelerate the Growth of the Market | Analysis by Industry Professionals," *Market Research Future*, May 24, 2018. [Online]. Available: Market Watch: https://www.marketwatch.com. [Accessed Jul. 23, 2019].

[7] J. L. Flaubert, C. M. Spicer, A. M. Jetta, Eds., *The Promise of Assistive Technology to Enhance Activity and Work Participation*, *National Academies Press*, 2017.

[8] F. Cordella, A. L. Ciancio, R. Sacchetti, A. Davalli, A. G. Cutti, E. Guglielmelli, and L. Zollo, "Literature Review on Needs of Upper Limb Prosthesis Users," *Frontiers in Neuroscience*, vol. 10, no. 209, 2016.

[9] A. H. Mohamad, B. T. Abdulbaqi, N. K. Jumaa, "Hand Motion Controlled Robotic Arm based on Micro-Electro-Mechanical-System Sensors: Gyroscope, Accelerometer and Magnetometer," *Communications on Applied Electronics*, vol. 7, no. 4, pp. 6–11, 2017.

[10] P. Neto, J. N. Pires, and A. P. Moreira, "Accelerometer-Based Control of An Industrial Robotic Arm," *RO-MAN 2009 - The 18th IEEE International Symposium on Robot and Human Interactive Communication*, pp. 1192–1197, 2019.

[11] P. J. Kyberd and A. Poulton, "Use of Accelerometers in the Control of Practical Prosthetic Arms," *IEEE Transactions on Neural Systems and Rehabilitation Engineering*, vol. 25, no. 10, pp. 1884–1891, 2017.

[12] J. E. Sanders, R. A. Miller, D. N. Berglund, and S. G. Zachariah, "A modular six-directional force sensor for prosthetic assessment: A technical note," *The Journal of Rehabilitation Research and Development*, vol. 34, no. 2, pp. 195–202, 1997.
[13] E. S. Neumann, J. Brink, K. Yalamanchili, and J. S. Lee, "Use of a load cell and force–moment curves to compare transverse plane moment loads on transtibial residual limbs: A preliminary investigation," *Prosthetics and Orthotics International*, vol. 38, no. 3, pp. 253–262, 2014.
[14] D. M. Stefanescu, *Handbook of Force Transducers: Principles and Components*, Berlin: Springer-Verlag GmbH, 2011.
[15] R. R. Fletcher, "Force Transduction Materials for Human-Technology Interfaces," *IBM Systems Journal*, vol. 35, no. 3.4, pp. 630–638, 1996.
[16] Kono, Masashi & Taura, Tetsuya & Sunaga, Hiroshi & Kimura, Keigo & Suzuki, Takahide & Morimura, Masanao & Okano, Haruki & Iwasaki, Masami & Takuno, Hiroyuki & Suzuki, Masamitsu & Kobayashi, Haruo. A High-Precision AC Wheatstone Bridge Strain Gauge: *IEICE Transactions on Electronics*. 2006; J91-C.
[17] T. G. Beckwith, R. D. Marangoni, and J. H. Lienhard V, *Mechanical Measurements*, 5th ed. Prentice Hall, 1993.
[18] A. Wolfenden, *Dynamic Elastic Modulus Measurements in Materials*, 17th ed. West Conshohocken, PA: American Society for Testing and Materials, 1990.
[19] F. Levinzon, *Piezoelectric Accelerometers with Integral Electronics*, Istanbul, TR: Springer International Publishing, 2015.
[20] A. Cranny, D. P. J. Cotton, P. H. Chappell, S. P. Beeby, and N. M. White, "Thick-film Force and Slip Sensors for A Prosthetic Hand," *Sensors and Actuators A: Physical*, vol. 123–124, pp. 162–172, 2005.
[21] A. M. Almassri, W. Z. Wan Hasan, S. A. Ahmad, A. J. Ishak, A. M. Ghazali, D. N. Talib. and C. Wada, "Pressure Sensor: State of the Art, Design, and Application for Robotic Hand," *Journal of Sensors*, 2015.

Corresponding author:
Tran Dang Khoa
Ho Chi Minh City University of Technology and Education
Email: tdkhoa@hcmute.edu.vn